J. Membrane Biol. 108, 273–282 (1989)

The Journal of
Membrane Biology

Inhibition of Electrical Coupling in Pairs of Murine Pancreatic Acinar Cells by OAG and Isolated Protein Kinase C

R. Somogyi, A. Batzer, and H.-A. Kolb
University of Konstanz, Faculty of Biology, D-7750 Konstanz, Federal Republic of Germany

Summary. Gap junctional coupling was studied in pairs of murine pancreatic acinar cells using the double whole-cell patch-clamp technique. During stable electrical coupling, addition of OAG (1-oleoyl-2-acetyl-*sn*-glycerol) induced a progressive reduction of the junctional conductance to the detectable limit (~3 pS). Prior to complete electrical uncoupling, various discrete single channel conductances between 20 and 100 pS could be observed. Polymyxin B, a potent inhibitor of the protein kinase C (PKC) system, completely suppressed OAG-stimulated electrical uncoupling. Dialysis of cell pairs with solutions containing PKC, isolated from rat brain, also caused electrical uncoupling. The presence of 0.1 mM dibutyryl cyclic AMP and 5 mM ATP in the pipette solution, which serves to stabilize the junctional conductance, did not suppress the effects of OAG or isolated PKC. We conclude that an increase of protein kinase C activity leads to the closure of gap junction channels, presumably via a PKC-dependent phosphorylation of the junctional peptide, and that this mechanism is dominant over cAMP-dependent upregulatory effects in the experimental time range (≤1 hr). A correlation of the observed single channel conductances with the appearance of channel subconductance states or various channel populations is discussed.

Key Words electrical coupling · gap junction · double whole cell patch clamp · cAMP · protein kinase C · OAG

Introduction

Protein kinases appear to play an integral role in stimulus secretion coupling in pancreatic acinar cells. Different kinase activities have been demonstrated in pancreatic acini, including a cAMP-dependent protein kinase, a Ca^{2+}-calmodulin dependent kinase, and protein kinase C (Burnham & Williams, 1984*a*; Noguchi et al., 1985). They appear to be differentially activated by secretagogues such as secretin and vasoactive intestinal peptide, which increase the production of cAMP, or cholecystokinin and cholinergic agents, which lead to a G-protein mediated activation of phospholipase C, resulting in an elevation of the intracellular Ca^{2+} concentration and protein kinase C activity (Burnham & Williams, 1984*b*; Merritt et al., 1986; Ishizuka et al., 1987; Schnefel et al., 1988). Activation of PKC and a concomitant increase of amylase release could also be induced by phorbol esters and diacylglycerol (Wooten & Wrenn, 1984; Merritt & Rubin, 1985).

Intercellular communication via gap junctions has been implied in the control of secretion. Uncoupling of pancreatic acinar cells with heptanol has been shown to increase basal and secretin-mediated amylase release, while carbachol-induced secretion remains unaffected (Meda et al., 1987). Also, in addition to activating PKC, cholinergic agents like carbachol lead to uncoupling (Iwatsuki & Petersen, 1979), which could explain why heptanol has no additional effect on carbachol-induced secretion. Secretion is not investigated in the present work. We attempt here to clarify whether direct activation of PKC affects the permeability of gap junctions in pancreatic acinar cells.

Inhibitory effects of phorbol esters and diacylglycerol on gap junctional communications have recently been reported for cultured cells (Murray & Fitzgerald, 1979; Yotti, Chang & Trosko, 1979; Gainer & Murray, 1985; Yada, Rose & Loewenstein, 1985) as well as for freshly isolated cells (Randriamampita et al., 1988). Furthermore, evidence for the in vitro phosphorylation of lens intrinsic membrane protein and the 27-kD gap junction subunit of rat liver by protein kinase C is available (Lampe et al., 1986; Takeda et al., 1987). Since the subunit of rat liver gap junctions is broadly homologous with the pancreatic junctional peptide, based on the subunit antigenic properties (Dermietzel et al., 1984; Beyer, Paul & Goodenough, 1987), it seems plausible to assume an analogous effect of PKC on gap junctions of pancreatic acinar cells.

In this paper we show that exposure of cell pairs to OAG (1-oleoyl-2-acetyl-*sn*-glycerol), an an-

Table. Composition of buffers used for isolation of protein kinase C[a]

	A	B	C	D	E
Tris-HCl	20 mM	20 mM	20 mM	10 mM	20 mM
Glycerol	40%	5%	5%	5%	5%
DTE	5 mM	2.0 mM	1.0 mM	1.0 mM	1.0 mM
EDTA	2 mM	0.5 mM	0.5 mM	0.25 mM	0.25 mM
EGTA	5 mM	0.5 mM	0.5 mM	0.25 mM	0.25 mM
cAMP	50 μM	20 μM	—	—	—
NaCl	—	—	1.5 M	—	100 mM

[a] All solutions are based on a formula containing 1 μM Pepstatin A (Sigma) and 10 U/ml aprotinin (Trasylol, Bayer, Leverkusen, FRG), at pH 7.5.

alogue of the endogenous activator of PKC, diacylglycerol, leads to electrical uncoupling. This effect can be eliminated by addition of polymyxin B (PMB). PMB putatively inhibits PKC by interacting with phosphatidylserine (Mazzei, Katoh & Kuo, 1982). Moreover, for the first time, purified PKC is employed to study the effect of increased PKC activity on junctional coupling. After the junctional conductance of well-coupled cell pairs had been reduced by OAG or PKC, stepwise changes of the junctional current could be examined. The discrete conductances can be compared to those observed previously during spontaneously occurring uncoupling (Somogyi & Kolb, 1988*a*) and to conductances found in lacrimal gland (120 pS; Neyton & Trautman, 1985), in embryonic heart (135–165 pS; Veenstra & De Haan, 1986, 1988), in neonatal heart (53 pS; Burt & Spray, 1988) and in *Xenopus* myolomal muscle cells (114 pS; Chow & Young, 1987). It will be discussed whether the examined conductances reflect subconductance states of one channel or altogether different channel types.

Materials and Methods

Cell Preparation

Acinar cells were obtained through collagenase digestion of the freshly isolated pancreas of a two to three month-old male NMRI mouse (Somogyi & Kolb, 1988*a*). Briefly, the mechanically dissociated pancreatic tissue was digested in KRH-Ca^{2+} (Krebs-Ringer-HEPES) medium with 200 units type III collagenase (Worthington, Freehold, NJ) for 15 min. An incubation in calcium-free KRH-EGTA for 15 min followed. In the last step the tissue was dissociated into single cells, pairs, and small aggregates by treatment with 300 units collagenase (as above) in KRH-Ca^{2+} for 1 hr. During all incubations the tissue suspension was rotated in a water bath at 37°C. Cells were stored at 4°C in BME (Basal Medium Eagle)-Hanks (SIGMA, St. Louis, MO) buffered with 25 mM HEPES at pH 7.4, and used up to 36 hr after isolation.

Isolation of Protein Kinase C

All subsequent operations were carried out between 0 and 4°C. Four rat brains (total weight: 8.5 g) were placed in 42.5 ml buffer A (*see* Table for buffers) and homogenized with a Sorvall-Polytron mixer at maximal speed (three times, 30 sec each). The homogenate was centrifuged at 100,000 × *g* for 45 min. Subsequently the supernatant was filtered through a layer of glass wool and applied to a DE-52 (Whatman) column (length: 15 cm, diameter: 1.4 cm), equilibrated in buffer B (*see* Table). After washing the column with 250 ml of buffer B, elution took place using an 8-hr linear salt gradient from 0 to 300 mM NaCl in buffer B. Fractions of 4 ml were collected and assayed for PKC activity.

The PKC peak fractions were pooled and the conductivity was adjusted to that of buffer C (*see* Table) by adding NaCl. This solution was applied to a phenyl-sepharose (Pharmacia) column (length: 15 cm, diameter: 1 cm) equilibrated in buffer C. After washing with 200 ml of buffer C, a two-step elution of the column by linear salt gradients in buffers C and D followed: step 1 from 1.5 M to 400 mM NaCl for 3 hr and step 2 from 400 to 0 mM NaCl for another 3 hr. Fractions of 1.5 ml were collected and assayed for PKC activity.

The fractions containing peak PKC activity were precipitated by dialysis against a 4 M ammonium sulfate solution at room temperature. After 2 hr of dialysis, the precipitate was centrifuged for 10 min at 10,000 × *g* and taken up in 1 ml of buffer E (*see* Table). The solution was then applied to a 90-ml Superose 12-prep grade FPLC column (Pharmacia), equilibrated in buffer E. Fractions of 0.9 ml were collected at a flow rate of 0.3 ml/min and assayed for PKC activity.

The peak PKC activity fractions, corresponding to a purification factor of 650 as compared to the primary brain extract, were pooled and dialysed for 1 hr in pipette control buffer (*see* electrolyte solutions and media) containing 20% glycerol. This solution, referred to as PKC stock, was stored n 100 μl aliquots in liquid nitrogen. To determine whether freezing and prolonged storage affect PKC activity, an aliquot of enzyme was thawed and assayed after three months. A phosphorylation rate of 27.3 nmol phosphate/(min · mg protein) was assayed, demonstrating no loss of activity.

Assay of Protein Kinase C Activity

Protein kinase C was routinely assayed by measuring the incorporation of ^{32}P from (gamma ^{32}P) ATP into Histone III-S (Sigma). The reaction mixture (total volume 30 μl) contained 50 mM Tris/HCl at pH 7.5, 0.67 mg/ml of Histone III-S, 5 mM $MgCl_2$, 0.5 mM $CaCl_2$, 0.067 mg/ml phospholipid (85% phosphatidylserine, Sigma B1627), 1.3 μg/ml diolein (85% 1,3 isomer, Sigma D8894), 0.4 mM (gamma ^{32}P) ATP (0.25 MBq/mol) and the enzyme preparation to be assayed. Phospholipid and diolein were sonicated for 30 sec before use. Standard incubation time was 30 min at room temperature. Fractions were assayed with and without phospholipid/diolein in order to identify protein kinase C. The assay was performed according to the procedure of Thalhofer et al. (1988).

In order to characterize PKC activity under conditions comparable to the double whole cell experiments, assays were performed at 10^{-7} M free Ca^{2+}, with and without diolein and phospholipid, respectively. The reaction mixture at which maxi-

mal activity (19.7 nmol phosphate/(min · mg protein)) was measured contained: 18.6 mM Na^+, 43.3 mM Cl^-, 3.3 mM glucose, 10 mM HEPES, 5 mM EGTA, 1.7 mM ATP, 0.03 mM cAMP, 10^{-7} M free Ca^{2+}, 1 mM free Mg^{2+}, 0.6 mg/ml Histone III-S, 0.067 mg/ml phospholipid, 1.3 μg/ml diolein, 0.4 mM (gamma ^{32}P) ATP. If diolein or phospholipid was omitted, phosphorylation rates of 13.9 nmol phosphate/(min · mg protein) and 8.9 nmol phosphate/(min · mg protein) were obtained, respectively. While no diolein or phospholipid was added, a basal activity of 6.1 nmol phosphate/(min · mg protein) was assayed. The residual activity was probably due to proteolysis during the preparation, which renders the enzyme into a permanently active conformation (Inoue et al., 1977).

Recording the Junctional Conductance

Double whole-cell experiments (Neyton & Trautmann, 1985) were conducted at room temperature as described previously (Somogyi & Kolb, 1988*a*). After allowing the cells to settle in a perfusion chamber (volume 200 μl) for 10 min, a cell pair was selected and the double whole-cell configuration established. Rectangular voltage pulses of 100 Hz were applied immediately after sealing in order to check seal and input resistance. Junctional current records were obtained by applying a rectangular voltage pulse of varying amplitude to one cell, while the other was held constant, and reversing the order of the pulsed and steady cell once every minute to exclude one-sided artifacts.

Data Analysis

Data were recorded and evaluated as described in Somogyi and Kolb (1988*a*). Patch-clamp currents were amplified using two LIST EPC-7 amplifiers and recorded on a RACAL Store 4 DS *fm* tape recorder at a cutoff frequency of 2.5 kHz, or 20 kHz for input resistance test pulses. Current-voltage data were evaluated by visual inspection of records charted using a GOULD model 2400 four-channel brush recorder, and entered into a Hewlett Packard 9825 desktop computer for calculation and presentation.

The junctional conductance was calculated by dividing the respective differences of the junctional current, ΔI_j, and the junctional potential difference, ΔV_j, before and after a voltage pulse (Neyton & Trautmann, 1985). To correct ΔV_j by the voltage drop across the electrodes, the series resistances of the pipettes $R_i (i = 1,2)$ were determined by the amplitude of the slow component of the exponential current relaxation after a voltage jump. The junctional voltage corrected by R_i approaches the applied potential differences between the two pipettes while g_j decreases to the single-channel level, minimizing the error of R_i in the determination and ΔV_j.

In order to obtain an estimate of the nonjunctional membrane resistance $R_{mi} (i = 1,2)$, the voltage jump difference of the stimulated cell was divided by the difference between the current sum of the stimulated and unstimulated cell before and after the voltage jump.

If cell 1 was pulsed and cell 2 held at a constant potential, the junctional current difference before and after a voltage jump was taken to be: $\Delta I_j = \Delta I_2(1 + R_2/R_{m2})$. For consistency, the sign of the junctional parameters (V_j and I_j) shown in *I-V* plots is always respective to system 1, i.e., for $I_j = I_2$ the actually measured sign is reversed. Experiments with values of $r \equiv R_i/R_{mi} \geq 0.1$ ($i = 1,2$) were rejected. r was constantly monitored in each experiment and included in the calculation of ΔI_j.

To demonstrate the time dependence of g_j from experiments performed under comparable conditions, the means and standard deviations (SD) of the combined data sets were calculated in intervals of 4 min. The mean junctional conductance values were then displayed (denoted by $\overline{g_j}$) with their respective standard deviations, of which only the positive SD bar is shown. The time axis zero always corresponds to the point at which the double whole-cell seals were formed.

For the evaluation of single-channel properties, records were chosen in which discrete steps of the junctional current could be observed in both records. The trace of the cell held close to the membrane reversal potential was used for analysis, since it contained less noise.

Amplitude histograms were obtained using the histogram function of a Hewlett Packard 5420A digital signal analyzer. Records were filtered at 40 Hz (eight pole Butterworth, Krohn Hite-Mod. 3342). Sampling frequencies were always set well above the cutoff frequency (*see also* Somogyi & Kolb, 1988*a*).

Electrolyte Solutions

A high KCl buffer containing ATP and *db*-cAMP, *p*Ca 7 at pH 7.4, was used as the pipette control solution: 145 mM K^+, 10 mM Na^+, 127 mM Cl^-, 0.1 μM Ca^{2+}_{free} (3.3 mM Ca^{2+}_{tot}), 1.0 mM Mg^{2+}_{free} (6.0 mM Mg^{2+}_{tot}), 10 mM glucose, 10 mM HEPES, 5 mM EGTA, 5 mM ATP^{2-}, 0.1 mM *db*-cAMP. ATP and *db*-cAMP were purchased from Sigma (St. Louis, MO), HEPES from Serva (Heidelberg, FRG). The Ca^{2+}_{free} concentration was determined as in Somogyi and Kolb (1988*a*). NaCl-BS was used as the bath medium: 145 mM NaCl, 5 mM KCl, 1 mM $CaCl_2$, 1 mM $MgCl_2$, 10 mM HEPES, 10 mM EGTA, pH 7.4.

OAG (1-oleoyl-2-acetyl-*sn*-glycerol, Sigma, St. Louis, MO) was stored under nitrogen at −20°C as a stock solution of 20 mg/ml in DMSO (dimethyl sulfoxide). Before application to cells, OAG/DMSO was diluted in NaCl-BS to a final concentration of 100 or 200 μg/ml OAG (0.5 or 1% DMSO) and sonified for 5 min under nitrogen. PMB (polymyxin B sulfate, 7700 USP units/mg, Sigma, St. Louis, MO) was dissolved in NaCl-BS and added to the OAG-containing bath buffers in the concentration of 240 or 120 μg/ml. For control experiments, or prior to perfusion of OAG or OAG/PMB solution, the cells were bathed from the start in NaCl-BS containing 0.5 or 1% DMSO, depending on which OAG concentration was intended to be used.

In experiments employing purified PKC, the PKC stock was diluted by a factor of four or eight in pipette control. About 10 μl of this solution was used to fill both pipette tips, the rest of the pipette volume containing unmodified pipette control. A similar dilution of remaining PKC dialysis buffer (not containing protein) in pipette control was used in control experiments.

Results

Effect of OAG and Isolated PKC on Electrical Coupling

Electrical coupling of freshly isolated murine pancreatic cells was monitored in the double whole-cell configuration. In a previous paper (Somogyi & Kolb, 1988*a*), it had been shown that addition of 0.1 mM *db*-cAMP and 5 mM ATP to the pipette solution

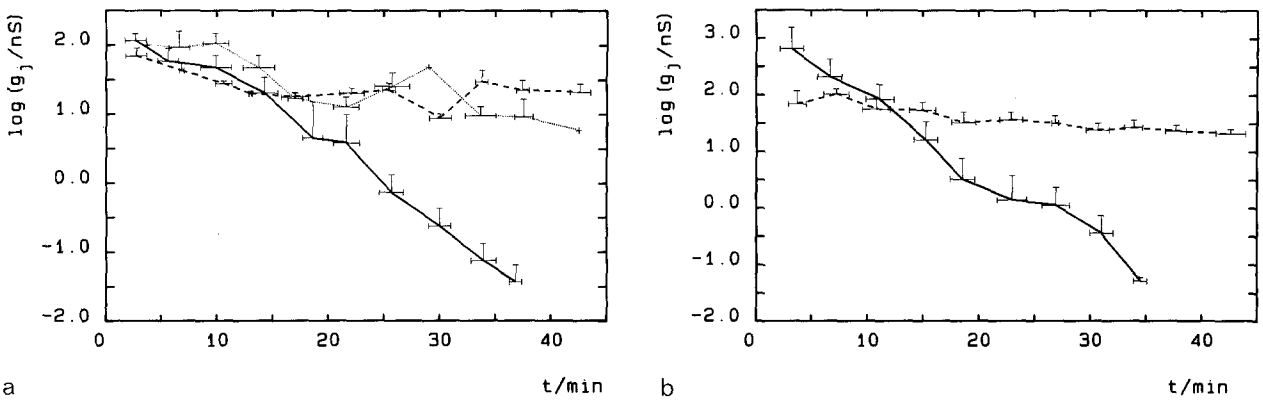

Fig. 1. (*a*) Uncoupling induced by 1-oleoyl-2-acetyl-*sn*-glycerol (OAG) and inhibition thereof by polymyxin B (PMB). The time course of the mean junctional conductance ($\overline{g_j} \pm$ SD) of four experiments, in which OAG served as an uncoupling agent, is shown by the solid line. OAG was added to the bath medium 5 min after the beginning of an experiment in the concentrations of 200 μg/ml ($n = 2$) and 100 μg/ml ($n = 2$), corresponding to 1 and 0.5% dimethyl sulfoxide (DMSO) in the bath, respectively (*see* Materials and Methods). The broken line represents two control experiments in which 1% DMSO was included in the bath solution throughout the experiment. In three experiments using the protein kinase C inhibitor PMB (dotted line), a solution of 200 μg/ml OAG (1% DMSO), supplemented by 240 μg/ml PMB ($n = 2$) or 120 μg/ml PMB in an additional experiment, was used to replace the bath medium 5 min after initiation of the recording. (*b*) Uncoupling induced by purified protein kinase C (PKC). The solid line connects the mean junctional conductance data sets of four experiments in which PKC was added to the pipette medium. In three of these experiments, the PKC stock was diluted by a factor of eight (2.5% glycerol in bath and pipette), while in one a fourfold dilution was used (5% glycerol in bath and pipette; *see* Materials and Methods). The broken line represents the time course of $\overline{g_j}$ of three control experiments. A fourfold dilution of protein-free, used dialysis buffer was employed as a control pipette solution in two experiments (5% glycerol in bath and pipette), while a 20-fold dilution was used in another experiment (1% glycerol in bath and pipette; *see* Materials and Methods).

was sufficient to maintain a stable junctional conductance, which could be recorded for over 60 min. For the following experiments, a pipette control solution (*see* Materials and Methods) yielding such stable electrical coupling was chosen.

After 5 min of recording under control conditions the NaCl-BS bath electrolyte was replaced by the same solution containing OAG (100–200 μg/ml; 0.5–1% DMSO). Figure 1*a* shows the corresponding time course of the mean junctional conductance ($\overline{g_j}$) of four different cell pairs. $\overline{g_j}$ decreases by more than three orders of magnitude within an exposure time of 30 min. To test whether the solvent DMSO affected junctional coupling, control experiments were performed in which 1% DMSO was added to the bath. No significant changes of $\overline{g_j}$ were observed under these conditions ($n = 2$, broken line, Fig. 1*a*).

In order to ascertain whether the effect of OAG is due to the specific activation of PKC, we investigated the combined action of OAG and polymyxin B. The latter amphipathic antibiotic has been determined to be a potent inhibitor of PKC activity being more than 100 times more specific for the PKC than for the Ca^{2+}/calmodulin system (Wrenn & Wooten, 1984). The dotted line in Fig. 1*a* shows the time course of $\overline{g_j}$ in three experiments in which a bath solution containing 200 μg/ml OAG, 1% DMSO and 120 μg/ml ($n = 1$) or 240 μg/ml ($n = 2$) PMB was employed. The figure indicates that PMB in these concentrations suppresses OAG-induced uncoupling.

As an alternative to the stimulation of endogenous PKC by OAG, PKC activity can also be elevated by intracellular introduction of this enzyme. We have therefore added isolated rat brain PKC to both pipette solutions to check if this also causes uncoupling. After enabling PKC to diffuse into both cells through the broken membrane patches, a progressive decrease of $\overline{g_j}$ could be observed (Fig. 1*b*). Since the PKC activity required stabilization by glycerol, which may cause cell swelling, the cells were preincubated for at least 15 min in NaCl-BS containing the same concentration of glycerol as the pipette PKC solution.

Control experiments were performed to assure that neither externally nor internally applied glycerol, nor residual components in the PKC buffer were responsible for uncoupling. Therefore, used dialysis buffer (not containing protein) was diluted with pipette control solution, analogously to the PKC experiments, while the bath solution was modified by the equivalent concentration of glycerol. The results show that under control conditions of up to 5% glycerol no significant effect on $\overline{g_j}$ could be observed within a time span of at least 45 min.

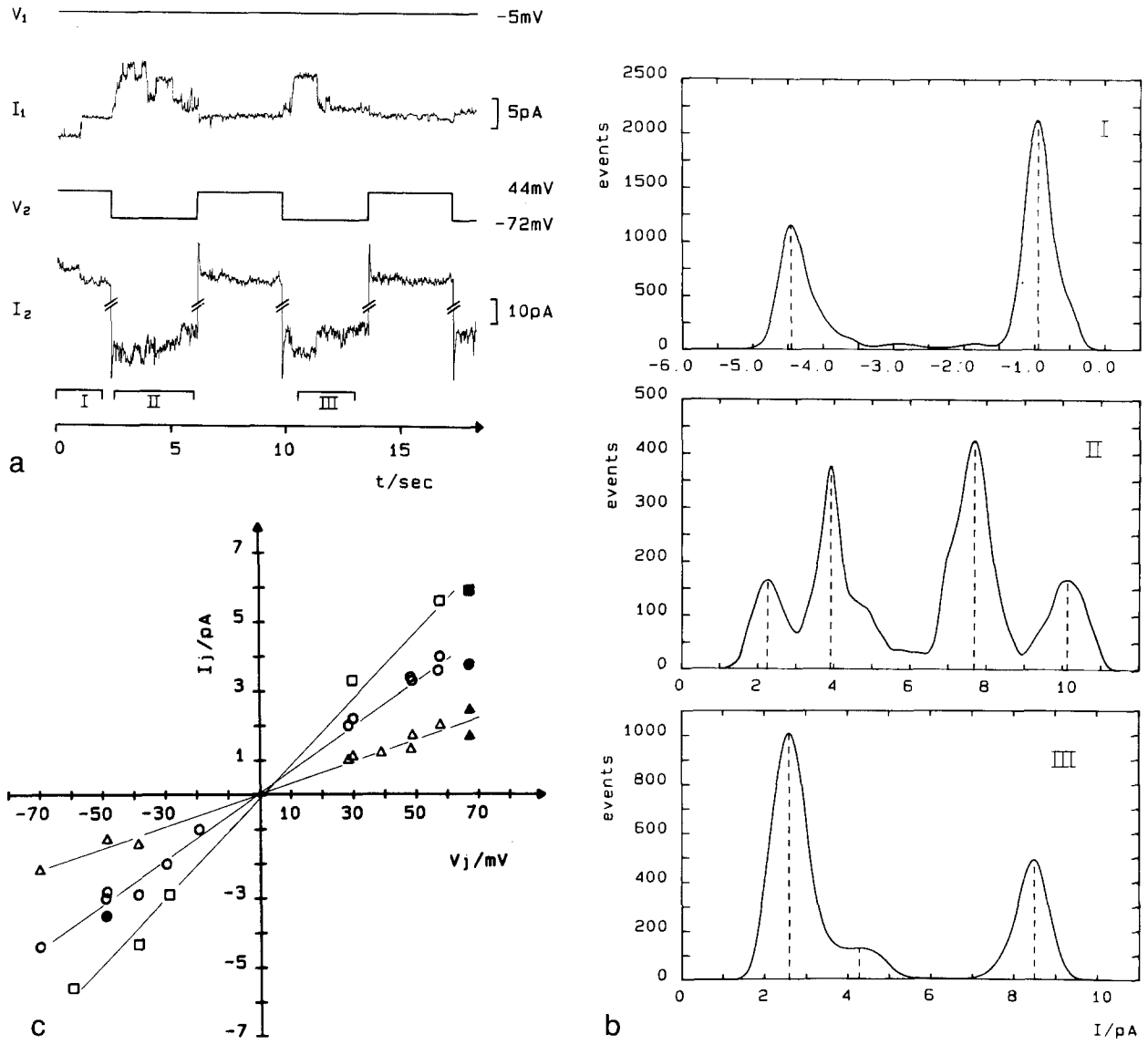

Fig. 2. (*a–c*). Single-channel analysis of the junctional conductance during uncoupling induced by 200 μg/ml OAG. (*a*) Junctional current record taken at $t = 37$ min into the recording. I_1 depicts the junctional current at alternating V_j of −49 and 67 mV (Materials and Methods). The counter-record, I_2, was cut along the current axis by 30 pA (*see* markings). (*b*) Histograms of the junctional current, I_1, marked by time axis brackets in *a*. Histogram *I* ($V_j = -49$ mV) shows the discrete channel amplitude of −3.5 pA as the distance between the maxima. Three current steps are depicted in histogram *II* ($V_j = 67$ mV), the peak distances counted starting at the first maximum being: $\Delta I_1 = 1.7$ pA, $\Delta I_2 = 3.8$ pA, $\Delta I_3 = 2.4$ pA. A large single current step followed by a smaller one in *a* is shown in histogram *III* ($V_j = 67$ mV), the current maxima differences corresponding to 5.9 and 1.7 pA. (*c*) *I-V* plot of observed conductances. Current voltage values taken between 35 and 40 min from the same experiment as above are shown. The filled symbols correspond to the values described in *a* and *b*. Three different slope conductances could be fitted by linear regression: $g_1 = 31.4 \pm 1.6$ pS, P_r(current zero potential) = −1.0 mV (triangles), $g_2 = 64.4 \pm 1.7$ pS, $P_r = -0.8$ mV (circles), $g_3 = 96.1 \pm 3.7$ pS, and $P_r = 1.1$ mV (squares). $R_1 = 11.8$ MΩ, $R_2 = 7.0$ mΩ, $R_{m1} = 1000$ MΩ, and $R_{m2} = 3000$ MΩ

Discrete Fluctuations of the Junctional Conductance in the Presence of OAG and Elevated PKC

Uncoupling following PKC activation enabled the analysis of junctional current fluctuations at low junctional conductances. Figure 2*a* shows the junctional current at 37 min after the start of one particular experiment in which 200 μg/ml OAG was employed. The upper current trace, I_1, shows the response of the steadily clamped cell 1 to potential changes in the coupled cell 2. The potential of cell 1 was held close to the resting potential at −5 mV, to minimize the contribution of the nonjunctional

membrane current. Therefore, I_1 closely agrees with the junctional current I_j. The current of the pulsed cell (lower trace) is larger since it contains a significant nonjunctional membrane current contribution on top of the junctional current at 44 and −72 mV pipette potential.

Within the trace of I_1 (Fig. 2*a*), steps of different amplitudes, which are also reflected in the noisier record of I_2, can be discriminated. In this and other experiments, current records within which single-channel opening or closing events could be distinguished were digitized for analysis in the time range of 3 to 5 min before total uncoupling. Due to the slow fluctuating kinetics and interspersed, extended closed periods of the channels, roughly 50 opening or closing events, could be analyzed in each experiment. Therefore, frequency histograms of the single-channel conductances were not suitable for clearly determining the channel-size frequency distributions or the voltage dependence on the single-channel level (no voltage dependence could be observed for the macroscopic junctional current).

Three different junctional current amplitudes, as shown in the amplitude histograms (Fig. 2*b*) of the record segments denoted by brackets, *I*, *II* and *III* in Fig. 2*a*, could be identified. The current amplitude values are marked by filled symbols in the corresponding *I-V* plot, showing a linear current voltage relationship (Fig. 2*c*). Linear regression reveals the following conductances: $g_{j1} = 31.4 \pm 1.6$ pS ($n = 11$), $g_{j2} = 64.4 \pm 1.7$ pS ($n = 14$), $g_{j3} = 96.1 \pm 3.7$ pS ($n = 6$). The corresponding zero current potentials are −1.0, −0.8 and 1.1 mV, respectively.

Single-channel conductances could also be identified in other experiments using OAG. One experiment showed a single-channel conductance of 89.2 ± 2.2 and 45.2 ± 1.2 pS (Somogyi & Kolb, 1988*b*). The identified junctional current fluctuations in the other experiments showed a large variability, ranging from conductances of 20 to 90 pS. As a general parameter, mean conductances of 64.7 ± 3.6 ($n = 26$) and 47.2 ± 4.4 pS ($n = 28$) could be derived in different experiments. Similar observations were made in the experiments using isolated PKC to induce uncoupling. In this case, a maximal conductance of 100.9 ± 2.8 pS ($n = 10$) could be determined as shown in the records and analysis presented in Fig. 3. Though variable, lower junctional conductance fluctuations were observed using this protocol, they could not be clearly correlated to a limited set of discrete conductances.

Discussion

We have shown that stimulation of freshly isolated pancreatic acinar cells by the diacylglycerol OAG causes gap junction channel closure in dialyzed cell pairs. To suppress spontaneous electrical uncoupling of the cells due to an interruption of cellular metabolism by washout of intermediary metabolites, ATP and cAMP were added to the pipette solution in all the experiments (Somogyi & Kolb, 1988*a*). Ca^{2+} was buffered at 10^{-7} M, a concentration at which PKC can be well activated by diacylglycerol in the presence of membrane lipids (Nishizuka, 1984), but which is not high enough to induce uncoupling independently, as demonstrated by the control experiments. The ongoing dialysis of the cells with this high capacity Ca^{2+} buffer (5 mM EGTA) should assure that no significant variations of the cytosolic Ca^{2+} concentration occur during the experiment. Though some loss of PKC from the cell to the pipette is expected before addition of OAG, putative translocation of endogenous kinase to the membrane after stimulation should stabilize PKC activity at an elevated level.

These results are similar to previous reports showing that intercellular communication could be inhibited when PKC was activated by diacylglycerol or phorbol esters either on cell lines (Yotti et al., 1979; Enomoto et al., 1981; Yancey et al., 1982; Fitzgerald et al., 1983; Davidson, Baumgarten & Harley, 1985; Enomoto & Yamasaki, 1985; Yada et al., 1985) or freshly isolated rat lacrimal glands (Randriamampita et al., 1988). The rate of the OAG-PKC mediated uncoupling is similar to those already reported (Yada et al., 1985; Randriamampita et al., 1988).

To exclude the possibility that the effect of OAG is due to an unspecific effect on the membrane, or is mediated by degradation products of diacylglycerol, we tested the combined action of OAG and polymyxin B. Polymyxin B, a cyclic polycationic peptide antibiotic, is a highly potent inhibitor of PKC (Wooten & Wrenn, 1984; Wrenn & Wooten, 1984). Our data show (Fig. 1*a*) that the uncoupling influence of OAG is completely inhibited by addition of 240 μg/ml polymyxin B.

A major finding of this paper is that dialysis of a cell pair with purified PKC leads to uncoupling, PKC-induced electrical uncoupling starts within the same time range as the dialysis fo the cells (3–6 min; Pusch & Neher, 1988). Since we expect dialysis of proteins such as PKC (mol wt ~80 kDa) to be slower than that of smaller molecules (about 50% of the pipette concentration of protein should be reached in the cell after 15 min, according to Pusch and Neher (1988)), only a small percentage of the pipette PKC concentration may be present in the cell during the onset of uncoupling, observed 5–10 min after the start of the experiment. Considering that high concentrations of PKC were employed, complete exchange was apparently not necessary to

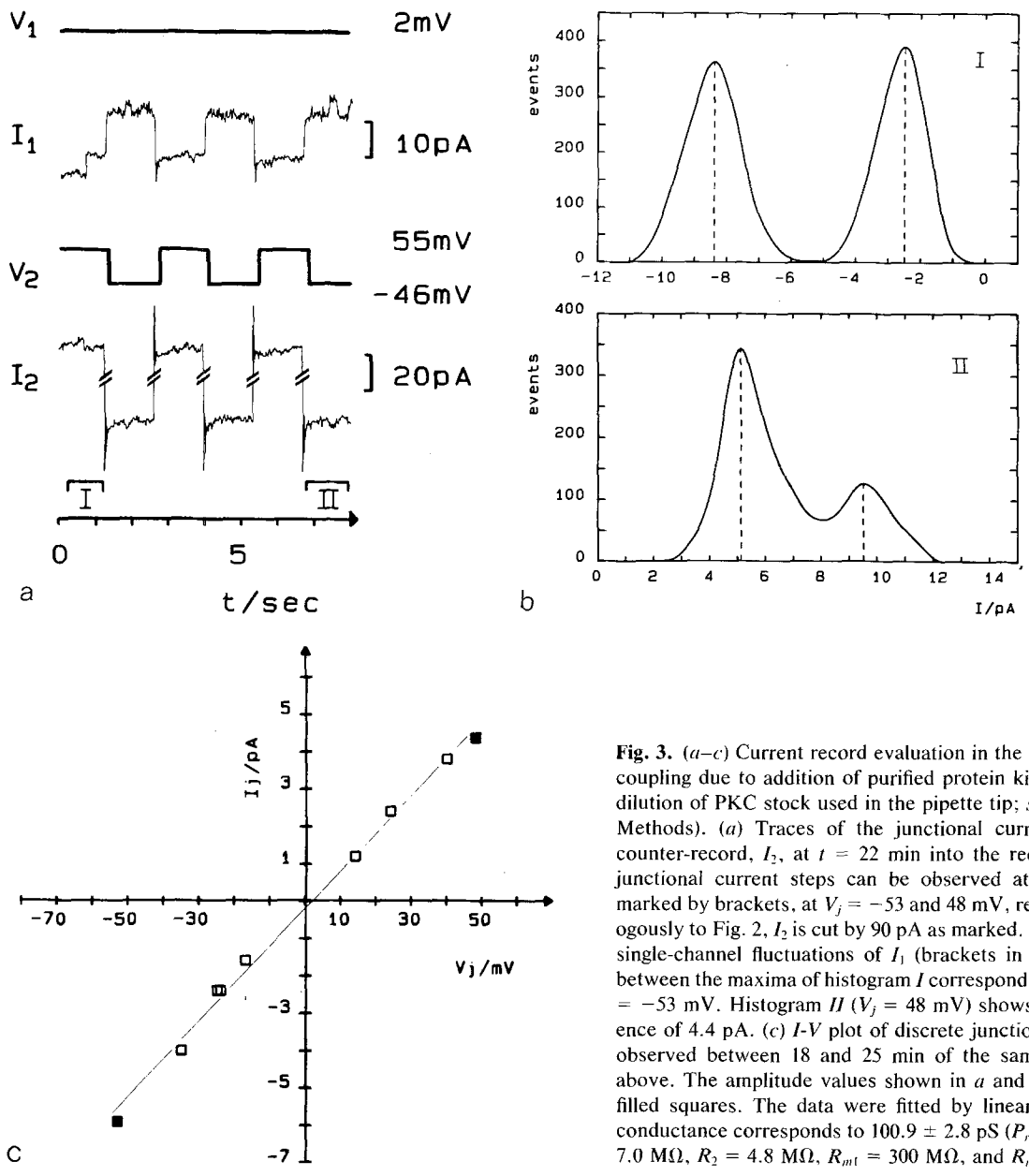

Fig. 3. (*a–c*) Current record evaluation in the final phase of uncoupling due to addition of purified protein kinase C (eightfold dilution of PKC stock used in the pipette tip; *see* Materials and Methods). (*a*) Traces of the junctional current, I_1, and the counter-record, I_2, at t = 22 min into the recording. Discrete junctional current steps can be observed at the time points marked by brackets, at $V_j = -53$ and 48 mV, respectively. Analogously to Fig. 2, I_2 is cut by 90 pA as marked. (*b*) Histograms of single-channel fluctuations of I_1 (brackets in *a*). The distance between the maxima of histogram *I* corresponds to −5.9 pA at V_j = −53 mV. Histogram *II* (V_j = 48 mV) shows a current difference of 4.4 pA. (*c*) *I-V* plot of discrete junctional current steps observed between 18 and 25 min of the same experiment as above. The amplitude values shown in *a* and *b* are marked by filled squares. The data were fitted by linear regression. The conductance corresponds to 100.9 ± 2.8 pS (P_r = 1.9 mV). R_1 = 7.0 MΩ, R_2 = 4.8 MΩ, R_{m1} = 300 MΩ, and R_{m2} = 1000 MΩ

raise PKC activity sufficiently to initiate uncoupling.

A question that may arise is whether the enzyme is expected to be active once it has entered the cell, since no effort has been made to elevate cellular diacylglycerol levels. Assays (*see* Materials and Methods) of this preparation in the presence of 10^{-7} M free Ca^{2+} have shown that, although PKC activity was maximal in the presence of diacylglycerol (DG) and phosphatidylserine (PS), it only diminished to 2/3 of maximal activity if DG was omitted, (in the presence of PS) and was still at a level of 1/3 of the maximal phosphorylation rate if both DG and PS were omitted in the test. Therefore, since PS, but not DG, is expected to be present in the cell membrane, specific PKC activity under double whole-cell conditions should lie between basal and PS stimulated levels.

Another aspect of the described experiments is the interaction of PKC with the cAMP-associated pathway. Since cAMP and ATP in the pipette were necessary to stabilize initial coupling (Somogyi & Kolb, 1988*a*), it is conceivable that the effect of PKC may be counteracted under these conditions. It has been shown that TPA-induced inhibition of junctional communication in Balb-c-3T3 cells could be eliminated by cAMP, an effect that requires *de novo* protein synthesis (Enomoto et al., 1984). Our

observations show that cAMP does not prevent the reduction of coupling induced by PKC. This result should be viewed in light of the fact that the double whole-cell configuration and the time span of recording should not permit additional protein synthesis.

As a model, we propose that cAMP-dependent phosphorylation of the junctional protein, directly or indirectly, is a precondition for it to be conducting, whereas additional phosphorylation by PKC leads to channel closure. This proposal would extend the established view of dual regulatory control of junctional permeability by upregulatory cAMP and downregulatory PKC-dependent phosphorylation (Yada et al., 1985). However, this regulatory mechanism may not be the same in all cells, e.g. in horizontal retina cells, cAMP depresses communication (Teranishi, Negishi & Kato, 1983; Piccolino, Neyton & Gerschenfeld, 1984; Lasater, 1987). But other mechanisms of gap junction closure besides direct PKC-induced phosphorylation of the connexon are conceivable. As an alternative, phosphorylation of other regulatory proteins may exert an inhibitory influence on coupling. A PKC-induced stimulation of another kinase such as the *src*-gene product, exhibiting tyrosine phosphorylation activity, is such a possibility (Azarnia et al., 1988).

The observation of single-channel fluctuations at a reduced junctional conductance allows the estimation of the channel radius from the determined discrete conductances. A simple, right cylindrical pore model serves as the basis of the following calculations (Hall, 1975; Hille, 1984). The pore conductance should, in this case, correspond to the inverse of the sum of the internal pore and pore-mouth access resistances. The expression for the channel conductance is derived as $g = (\sigma\pi r^2)/(l + 0.5\pi r)$, r being the pore radius, l the pore length and σ representing the solution conductivity inside the pore. We have measured the conductivity of the employed pipette control solution to be 1.65 S/m using a conductometer. This value could approximate the conductivity in the pore after dialysis of the cells. For a lower limit of the channel length of 18 nm (Caspar et al., 1977; Makowski et al., 1977; Zamphigi, Hall & Kreman, 1985), pore diameters of 0.66, 0.94, 1.14 and 1.2 nm have been calculated for conductances of 30, 60, 90 and 100 pS, respectively, which were analyzed from single-channel records of the experiments. These values of the pore diameter (d) are smaller, although in a comparable range, than those derived from electron microscopy ($d \leq 2$ nm; Unwin & Zampighi, 1980) and those estimated from dye transfer studies ($d \sim 1.6$–2.0 nm; Schwarzmann et al., 1981). Similar estimates for the heart gap junction channel size have lead to comparatively larger diameter values for the same conductance (60 pS), since the cytoplasmic resistivities of ventricular muscle cells, instead of the pipette electrolyte, i.e., the cell dialysis solution, were used in the calculations (Burt & Spray, 1988).

Finally, we would like to discuss the observed conductance steps in terms of unitary or intermediate conductances of gap junction channels. Discrete conductance fluctuations during PKC-mediated uncoupling have been observed between 20 and 100 pS. In all experiments, a maximal step of 90 to 100 pS could be identified, whereas lower frequently occurring conductances, e.g. 31, 64 pS, could vary in value from experiment to experiment. Similar observations have been made previously during spontaneous uncoupling of freshly isolated murine pancreatic acinar cells and cultured CHO cells, in which the analyzed discrete conductances were not the same in all experiments (Somogyi & Kolb 1988*a*). Two models could account for these results. Either the single channels making up a gap junction are *a priori* not homogeneous in their conductance, or PKC-mediated modulation, e.g. by phosphorylation, causes conformational changes in the channel, resulting in states of lowered conductance.

The existence of varying connexon subunits of 21 and 27 kD in the exocrine pancreas (Traub et al., 1988) suggests the existence of pores composed of different subunits, yielding homomeric or heteromeric structures. Such a model could explain the occurrence of different discrete conductance levels during uncoupling by the reduction of the open probability of initially mixed channel populations through the action of PKC. The evidence available to us does not support nor disprove the presence of mixed channel populations in a single gap junction plaque.

Since single-channel conductance values before PKC-induced uncoupling are not available, it cannot be conclusively shown that a PKC-mediated mechanism is responsible for the appearance of multiple discrete conductances. If the channel subunit contains a phosphorylation site for PKC, as in hepatocyte gap junctions (Takeda et al., 1987), it is conceivable that progressive conformational changes in the channel could take place as the subunits become consecutively phosphorylated. Such a process may not only affect the open probability, but also the inner diameter and shape of the individual pore. But this question remains elusive because single-channel parameters can only be analyzed when few channels are active, which may not be representative of the majority of channels previously conducting. Neither can a model be excluded that suggests the *a priori* presence of junctional channels with subconductance states, in which all

open states are more or less equally reduced in their frequency of occurrence by a PKC-dependent process.

The authors wish to thank Ms. G. Witz for her technical assistance in the data analysis, Ms. S. Kirsch for her help in the enzyme preparation, Mr. S. Galler for determining the free Ca^{2+} levels of the solutions, and Prof. W. Hofer for helpful discussions on the manuscript. This work was supported by the Sonderforschungsbereich 156 and research grant Ho 650/6 of the Deutsche Forschungsgemeinschaft.

References

Arzania, R., Reddy, S., Kmiecik, T.E., Shalloway, D., Loewenstein, W.R. 1988. The cellular *src* gene product regulates junctional cell-to-cell communication. *Science* **239:**398–401

Beyer, E.C., Paul, D.L., Goodenough, D.A. 1987. Connexin 43: A protein from rat heart homologous to gap junction protein from liver. *J. Cell Biol.* **105:**2621–2629

Burnham, D.B., Williams, J.A. 1984*a*. Activation of protein kinase activity in pancreatic acini by calcium and cAMP. *Am. J. Physiol.* **246:**G500–G508

Burnham, D.B., Williams, J.A. 1984*b*. Stimulus secretion coupling in pancreatic acinar cells. *J. Pediatr. Gastroenterol. Nutr.* **3:**S1–S10

Burt, J.M., Spray, D.C. 1988. Single-channel events and gating behavior of the cardiac gap junction channel. *Proc. Natl. Acad. Sci. USA* **85:**3431–3434

Caspar, D.L.D., Goodenough, D.A., Makowski, L., Phillips, W.C. 1977. Gap junction structures: I. Correlated electron microscopy and X-ray diffraction. *J. Cell Biol.* **74:**605–628

Chow, I., Young, S.H. 1987. Opening of single gap junction channels during formation of electrical coupling between embryonic muscle cells. *Dev. Biol.* **122:**332–337

Davidson, J.S., Baumgarten, I.M., Harley, E.H. 1985. Studies on the mechanism of phorbol ester-induced inhibition of intercellular junctional communication. *Carcinogenesis* **6:**1353–1358

Dermietzel, R., Leibstein, A., Frixen, U., Janssen-Timmen, U., Traub, O., Willecke, K. 1984. Gap junctions in several tissues share antigenic determinants with liver gap junctions. *EMBO J.* **3:**2261–2270

Enomoto, T., Sasaki, Y., Shiba, Y., Kanno, Y., Yamasaki, H. 1981. Tumor promoters cause a rapid and reversible inhibition of the formation and maintenance of electrical cell coupling in culture. *Proc. Natl. Acad. Sci. USA* **78:**5628–5632

Enomoto, T., Yamasaki, H. 1985. Rapid inhibition of intercellular communication between Balb-c-3T3 cells by diacylglycerol, a possible endogeneous functional analog of phorbol esters. *Cancer Res.* **45:**3706–3710

Enomoto, T.E., Martel, N., Kanno, Y., Yamasaki, H. 1984. Inhibition of cell communication between Balb/c3T3 cells by tumor promoters and protection by cAMP. *J. Cell. Physiol.* **121:**323–333

Fitzgerald, D.J., Knowles, S.E., Ballard, F.J., Murray, A.W. 1983. Rapid and reversible inhibition of junctional communication by tumor promoters in a mouse cell line. *Cancer Res.* **43:**3614–3618

Gainer, H.S.C., Murray, A.W. 1985. Diacylglycerol inhibits gap junctional communication in cultured epidermal cell: Evidence for a role of protein kinase C. *Biochem. Biophys. Res. Commun.* **126:**1109–1113

Hall, J.E. 1975. Access resistance of a small circular pore. *J. Gen. Physiol.* **66:**531–532

Hille, B. 1984. Ionic channels of excitable membranes. Sinauer Associates, Sunderland, MA

Inoue, M., Kishimoto, A., Takai, Y., Nishizuka, Y. 1977. Studies on a cyclic nucleotide-independent protein kinase and its proenzyme in mammalian tissues. *J. Biol. Chem.* **252:**7610–7616

Ishizuka, T., Ito, Y., Kajita, K., Miura, K., Nagao, S., Nagata, K., Nozawa, Y. 1987. Redistribution of protein kinase C in pancreatic acinar cells stimulated with caerulein or carbachol. *Biochem. Biophys. Res. Commun.* **144:**551–559

Iwatsuki, N., Petersen, O.H. 1979. Pancreatic acinar cells: The effect of carbon dioxide, ammonium chloride and acetylcholine on intercellular communication. *J. Physiol. (London)* **291:**317–326

Lampe, P.D., Bazzi, M.D., Nelsestuen, G.L., Johnson, R.G. 1986. Phosphorylation of lens intrinsic membrane proteins by protein kinase C. *Eur. J. Biochem.* **156:**351–358

Lasater, E.M. 1987. Retinal horizontal cell gap junctional conductance is modulated by dopamine through a cyclic AMP-dependent protein kinase. *Proc. Natl. Acad. Sci. USA* **84:**7319–7323

Makowski, L., Caspar, D.L.D., Phillips, W.C., Goodenough, D.A. 1977. Gap junction structures: II. Analysis of the X-ray diffraction data. *J. Cell Biol.* **74:**629–645

Mazzei, G.J., Katoh, N., Kuo, J.F. 1982. Polymyxin B is a more selective inhibitor for phospholipid-sensitive Ca^{2+}-dependent protein kinase than for calmodulin-sensitive Ca^{2+}-dependent protein kinase. *Biochem. Biophys. Res. Commun.* **109:**1129–1133

Meda, P., Bruzzone, R., Chanson, M., Bosco, D., Orci, L. 1987. Gap junctional coupling modulates secretion of exocrine pancreas. *Proc. Natl. Acad. Sci. USA* **84:**4901–4904

Merritt, J.E., Rubin, R.P. 1985. Pancreatic amylase secretion and cytoplasmic free calcium. Effects of ionomycin, phorbol dibutyrate and diacylglycerols alone and in combination. *Biochem. J.* **230:**151–159

Merritt, J.E., Taylor, C.W., Rubin, R.P., Putney, J.W., Jr. 1986. Evidence suggesting that a novel guanine nucleotide regulatory protein couples receptors to phospholipase C in exocrine pancreas. *Biochem. J.* **236:**337–343

Murray, A.W., Fitzgerald, D.J. 1979. Tumor promoters inhibit metabolic cooperation in coculture of epidermal and 3T3 cells. *Biochem. Biophys. Res. Commun.* **91:**395–401

Neyton, J., Trautmann, A. 1985. Single-channel currents of an intercellular junction. *Nature (London)* **317:**331–335

Nishizuka, Y. 1984. The role of protein kinase C in cell surface signal transduction and tumour promotion. *Nature (London)* **308:**693–698

Noguchi, M., Adachi, H., Gardner, J.D., Jensen, R.T. 1985. Calcium-activated, phospholipid-dependent protein kinase in pancreatic acinar cells. *Am. J. Physiol.* **248:**G692–G701

Piccolino, M., Neyton, J., Gerschenfeld, H.M. 1984. Decrease of gap junction permeability induced by dopamine and cyclic adenosine 3′:5′-monophosphate in horizontal cells of turtle retina. *J. Neurosci.* **4:**2477–2488

Pusch, M., Neher, E. 1988. Rates of diffusional exchange between small cells and a measuring patch pipette. *Pfluegers Arch.* **411:**204–211

Randriamampita, C., Giaume, D., Neyton, J., Trautmann, A. 1988. Acetylcholine-induced closure of gap junction channels

in rat lacrimal glands is probably mediated by protein kinase C. *Pfluegers Arch.* **412:**462–468

Schnefel, S., Banfic, H., Eckhardt, L., Schultz, G., Schulz, I. 1988. Acetylcholine and cholecystokinin receptors functionally couple by different G-proteins to phospholipase C in pancreatic acinar cells. *FEBS Lett.* **230:**125–130

Schwarzmann, G., Wiegandt, H., Rose, B., Zimmerman, A., Ben-Haim, D., Loewenstein, W.R. 1981. Diameter of the cell-to-cell junctional membrane channels as probe with neutral molecules. *Science* **213:**551–553

Somogyi, R., Kolb, H.A. 1988*a*. Cell-to-cell channel conductance during loss of gap junctional coupling in pairs of pancreatic acinar and Chinese hamster ovary cells. *Pfluegers Arch.* **412:**54–65

Somogyi, R., Kolb, H.A. 1988*b*. Modulation of gap junctional coupling in pairs of pancreatic acinar cells. *Ber. Bunsenges. Phys. Chem.* **92:**993–998

Takeda, A., Hashimoto, E., Yamamura, H., Shimazu, T. 1987. Phosphorylation of liver gap junction protein by protein kinase C. *FEBS Lett.* **210:**169–172

Teranishi, T., Negishi, K., Kato, S. 1983. Dopamine modulates S-potential amplitude and dye-coupling between external horizontal cells in carp retina. *Nature (London)* **301:**243–246

Thalhofer, H.P., Daum, G., Harris, B.G., Hofer, H.W. 1988. Identification of two different phosphofructokinase-phosphorylating protein kinases from *Ascaris suum* muscle. *J. Biol. Chem.* **263:**952–957

Traub, O., Look, J., Dermietzel, R., Brümmer, F., Hülser, D., Willecke, K. 1988. Comparative characterization of the 21kDa and 26kDa gap junction proteins in murine liver and cultured hepatocytes. *J. Cell Biol. (in press)*

Unwin, P.N.T., Zampighi, G. 1980. Structure of the junction between communicating cells. *Nature (London)* **283:**545–549

Veenstra, R.D., DeHaan, R.L. 1986. Measurement of single channel currents from cardiac gap junctions. *Science* **233:**972–974

Veenstra, R.D., DeHaan, R.L. 1988. Cardiac gap junction channel activity in embryonic chick ventricle cells. *Am. J. Physiol.* **254:**H170–H180

Wooten, M.W., Wrenn, R.W. 1984. Phorbol ester induces intracellular translocation of phospholipid/Ca^{2+} dependent protein kinase and stimulates amylase secretion in isolated pancreatic acini. *FEBS Lett.* **171:**183–186

Wrenn, R.W., Wooten, M.W. 1984. Dual calcium-dependent protein phosphorylation systems in pancreas and their differential regulation by polymyxin B1. *Life Sci.* **35:**267–276

Yada, T., Rose, B., Loewenstein, W.R. 1985. Diacylglycerol downregulates junctional membrane permeability. TMB-8 blocks this effect. *J. Membrane Biol.* **88:**217–232

Yancey, S.B., Edens, J.E., Trosko, J.E., Chang, C.-C., Revel, J.-P. 1982. Decreased incidence of gap junctions between chinese hamster V-79 cells upon exposure to the tumor promoter 12-0-tetradecanoyl phorbol-13-acetate. *Exp. Cell Res.* **139:**329–340

Yotti, L.P., Chang, C.C., Trosko, J.E. 1979. Elimination of metabolic cooperation in chinese hamster cells by a tumor promoter. *Science* **206:**1089–1091

Zampighi, G.A., Hall, J.E., Kreman, M. 1985. Purified lens junctional protein forms channels in planar lipid films. *Proc. Natl. Acad. Sci. USA* **82:**8468–8472

Received 20 October 1988; revised 17 January 1989